Three Mode Interactions as a Precision Monitoring Tool for Advanced Laser Interferometers

L Ju[1], C Zhao[1], D G Blair[1], S. Gras[2], S Susmithan[1], Q Fang[1] and C D Blair[1]
[1]The University of Western Australia
35 Stirling Highway, Crawley, WA 6009, Australia

[2]Kavli Institute for Astrophysics and Space Research,
Massachusetts Institute of Technology, 02139, USA

Email: li.ju@uwa.edu.au

Abstract. Many thousands of three-mode opto-acoustic interactions are expected to be observable in the advanced laser interferometer gravitational wave detectors now under construction. Each interaction represents a high-Q acoustic resonance interacting with high order optical modes inside the interferometer. This paper shows that this huge set of signals between 10-100kHz have high sensitivity to changes in the optical wavefronts within the interferometer and can be used to create a powerful probe of the entire interferometer. We show that 3MI signals can be used to monitor thermal distortions corresponding to wavefront changes ~3×10^{-12}m. Observations can be used at low optical power to predict parametric instabilities that could occur at higher power. In addition, the observed mode amplitudes could be used to control the interferometer operating point against slow environmental perturbations. Data on 80m cavities and modelling results are used to demonstrate the sensitivity of 3MI monitoring. Experimental observations on advanced interferometers are suggested as a means to turn 3MI monitoring into an effective tool.

1. Introduction

The first generation of large scale laser interferometer gravitational wave detectors reached their design sensitivity of h~$3 \times 10^{-23}/\sqrt{\text{Hz}}$, sufficient to detect rare astronomical events such as black holes mergers and neutron star coalescence events within 10-100Mpc [1]. Advanced detectors being constructed are aiming for sensitivity h ~ few $\times 10^{-24}/\sqrt{\text{Hz}}$, sufficient to observe the estimated population of neutron star coalescence events at a rate of tens of events per year.

This sensitivity improvement requires the use of high laser power inside the optical arm cavities to reduce shot noise, possibly in combination with optical squeezing [2]. High optical power leads to enhanced three mode opto-acoustic interactions (3MI) between the main cavity TEM_{00} mode, cavity transverse modes and acoustic modes of the suspended test mass mirrors. Rare interactions for which the opto-acoustic overlap factor is large [3,4] can achieve parametric gain R>1, which leads to parametric instability. Precise quantitative estimates are difficult because of uncertainties in material parameters, mirror parameters, optical alignments and losses [5]. Modelling to date indicates that a few acoustic modes per test mass could become unstable [6].

As discussed below, modelling also indicates that ~1800 acoustic modes per test mass (~7000 in total for 4 test masses) in the frequency range 10kHz to 150kHz, interacting with ~100 optical modes have parametric gain $>10^{-3}$ [6]. This gain is sufficient that the thermally excited acoustic modes can be easily observed by the beating signal in the transmitted or reflected light. Such signals are detectable using a spatially sensitive photodetector such as a quadrant photodetector (QPD). Because the cavity transverse

mode frequencies are very sensitive to mirror radius of curvature (RoC), which itself is tuned by absorbed laser light, and because the optical line widths are very narrow, the parametric gain (and hence the mode amplitude observed in the beating signal) is very sensitive to the interferometer operating conditions [7].

Three mode parametric interactions have been extensively studied in an 80m optical cavity at the Gingin High Optical Power Facility [8]. By thermally changing the radius of curvature of a cavity test mass mirror, using either a thermal compensation plate [9,10], a CO_2 laser [11, 12], or intrinsic self heating, 3MI signals have been observed with high signal to noise ratio. Three mode parametric instability in a free space optical cavity was first reported by Chen *et al*. [13], using a very low mass resonator in a tabletop experiment, but has still not been observed in a long baseline cavity with suspended test masses.

Many techniques for controlling parametric instability have been considered and investigated [14,15,16,17,18,19]. To some extent this work is hampered by lack of knowledge of which acoustic and optical modes are likely to be unstable, since this depends very strongly on unpredictable details such as thermal deformations and alignment variations. It would be very useful to have a means of diagnosing and predicting parametric instability before it occurs.

In this paper we consider the benefits of monitoring the very large number (~2800 at ~20W input power) of mostly low gain acoustic modes that will be detectable in advanced interferometers through 3MI. The monitoring could be useful in two ways. Firstly it can be used to obtain advance warning of parametric instabilities that are likely to occur at higher optical power. This can allow detector commissioners time to design specific control strategies for specific predicted instabilities. Secondly, the method can provide error signals which could be useful in determining alignments (particularly of transverse optical modes) and inhomogeneous temperature gradients that may otherwise be difficult to measure. This could be especially important because the enormous thermal memory of fused silica test masses (due to their long thermal relaxation time) means that they will almost never be in a state of dynamic equilibrium.

The proposed method relies on the fact that all acoustic modes are thermally excited and very well vibration isolated. For this reason the kT mean thermal energy of each mode can be treated as a calibration signal. As long as the mode energy is integrated over several relaxation times (typically integrating for 10-10^3 seconds) it provides a calibration signal with precision that increases with integration time. If the parametric gain approaches unity the calibration must be corrected by the parametric mode amplification which acts to increase the mode temperature by a factor $1/(1-R)$.

Advanced LIGO and Virgo already plan an extensive program of wavefront monitoring using Hartmann sensors to detect thermal distortions of test masses. The 3MI monitoring proposed here does not replace the use of Hartmann sensors, nor other sensors such as beam spot imaging and optical levers. At minimum it can provide early experimental prediction of parametric instability, but it has the possibility of providing much more useful information on all the interferometer optical cavities.

There are several factors that give 3MI monitoring an ability to diagnose multiple degrees of freedom in an interferometer including radii of curvature, inhomogeneous thermal distortion and optical alignments.

a) Each acoustic mode signal is the result of an opto-acoustic overlap between an acoustic mode and one or more high order transverse cavity modes. The overlap depends strongly on the high order mode position relative to the test mass, so transverse mode positions and orientations can be estimated.
b) Because parametric gain depends linearly on input laser power, monitoring of 3MI gain at low power can allow prediction of parametric instability at a higher power.
c) The high order transverse modes sample larger and different areas of the test mass compared with the main TEM_{00} beam. Hence 3MI monitoring can in principle detect thermally induced inhomogeneous radius of curvature variations.
d) The fact that all 3MI signals are associated with acoustic modes of individual test masses means that 3MI signals can be used for test mass thermometry The large acoustic mode frequency dependence on temperature, $(1/f)df/dT \sim 10^{-4}K^{-1}$ enables individual modes to be identified simply by observing the tuning when the thermal environment is altered (eg by warming the vacuum envelope of the test mass suspension tank). Thermal inhomogeneity can be estimated by comparing the 3MI gains of several acoustic modes.
e) As we show below, thousands of acoustic modes should be able to be monitored simultaneously. These signals are not all independent, because many have common associated transverse modes. However since many acoustic mode shapes can be inferred based on finite element modeling, unique solutions for important interferometer control parameters may be obtainable.

f) Parametric gain also depends on other interferometer components such as the beam splitter, the power and signal recycling mirrors, and power recycling cavity compensation plates, which all affect the transverse mode resonance. These components represent additional degrees of freedom that might be able to be measured through multiple 3MI monitoring.

In this paper new experimental results on a 76m fused silica optical cavity designed to achieve conditions similar to advanced LIGO and Virgo are presented showing that 3MI monitoring is very sensitive to mirror thermal deformations due to absorbed cavity power. New results derived from modelling of full scale advanced interferometers are presented that show that for typical advanced interferometer conditions 3MI monitoring has exceptional sensitivity to wavefront distortions ~ $10^{-6}\lambda$. We show that 3MI monitoring can identify modes that will become unstable at higher optical power in single cavities, and show that 3MI monitoring is very sensitive to thermal conditions and to beam spot position.

While demonstrating the intrinsic sensitivity available we emphasise that none of the modeling takes into account the asymmetric imperfections in the 8 independent optical elements mentioned in point f) above that play a role in each 3MI. The usefulness of 3MI monitoring will depend on the stability of measurements, and quality of finite element models, and the ability to invert the data to define unique control parameters. Thus we emphasize the importance of experimental investigation of the 10-100kHz frequency band of advanced interferometers with view to developing 3MI monitoring as a rich diagnostic resource.

First we will review the theory that underpins this work. Then we will present modelling results, followed by experimental results. Finally we will suggest future experimental investigations.

2. Theory of three mode interactions and predictions for Advanced detectors

In an optical cavity, the thermal motion of a test mass internal mode scatters the cavity TEM_{00} mode into higher order transverse modes TEM_{mn} (m and n are the mode number). The optical modes in turn interact with the test mass via the radiation pressure produced by the beating of the carrier and the transverse mode. Because this interaction involves 2 optical modes—the TEM_{00} and TEM_{mn} modes and one acoustic mode, it is called a three mode parametric interaction. The process can lead to either parametric cooling of the acoustic mode or parametric amplification (heating) of the acoustic mode. The gain of the 3-mode parametric interaction is given by [3]

$$R = \frac{P}{M\omega_0\omega_m^2 L^2}\frac{\Lambda}{1+(\Delta\omega_s/\delta)^2}Q_0Q_1Q_m \quad . \tag{1}$$

Here P is the laser power, Q_0, Q_1, and Q_m are the quality factors of the two optical modes and the acoustic mode of the test mass, M is the effective mass of the test mass, ω_0 and ω_m are the frequencies of the cavity and the test mass acoustic mode respectively, L is the length of the cavity, δ is the half width of the high order mode. The factor Λ is the mode shape overlap integral [3], describing how well the acoustic mode shape matches the optical mode shape. The factor $\Delta\omega_s=\Delta\omega-\omega_m$, where $\Delta\omega$ is the frequency difference between the TEM_{00} mode, ω_0, and the high order mode ω_a, is given by

$$\Delta\omega = \omega_0 - \omega_a = \frac{c}{L}(m+n)\arccos\left(\pm\sqrt{\left(1-\frac{L}{R_1}\right)\left(1-\frac{L}{R_2}\right)}\right). \tag{2}$$

Here R_1 and R_2 are the radii of curvature of the end mirrors of the cavity. The ± sign depends on the cavity configuration.

Equation (1) is simplified, considering only the Stokes process where parametric amplification or instability processes occur with only one higher order optical mode taken into account. There are a roughly equal number of negative gain modes that can be equally useful for obtaining interferometer information but which will not cause instability. Furthermore in many cases multiple higher modes can interact with a single acoustic mode, so that the gain R is a summation over several 3MI processes [20].

It can be seen from equation (1) that in a high optical power cavity with high optical Q factors, when the frequency condition $\omega_0-\omega_a=\omega_m$ is met and the high order mode has high spatial overlap with the acoustic mode, the parametric gain can be large, leading to parametric instabilities where the acoustic mode amplitude will ring up exponentially. The overlap parameter is a key parameter here because it is sensitive to the position of the optical cavity transverse mode relative to the acoustic mode which is fixed in the test mass.

Small motion of the beam position or distortion of the transverse mode can change the parametric gain strongly.

Gras *et al* [6] analysed parametric instabilities in advanced gravitational wave detectors and showed that there would always be a few unstable modes in each test mass at full operating power unless the parametric instability is suppressed. Unfortunately 3MI is so sensitive to system parameters such as laser spot position, mirror radius of curvature, and actual mode shapes and positions (which can be significantly distorted by mirror thermal distortions) that the specific modes that will become unstable are almost impossible to predict in advance. However it is also this sensitivity to optical parameters that enables 3MI monitoring to be a useful tool.

3. Modelling Studies

Figure 1. An example of acoustic modes showing the variability of parametric gain in a 4km dual recycling advanced gravitational wave detector configuration with fused silica ITM RoC=1971m and ETM RoC=2191m []. The acoustic modes are clustered in strips corresponding to cavity transverse mode offset frequencies. The cumulative number of acoustic modes (which is roughly the same across large range of RoC) is also given. All modes with gain > 10-3 should be easily detectable with a multi-element photodetector as discussed in text.

shows a snapshot of acoustic modes of a test mass in a 4km dual recycling gravitational wave configuration with a particular radius of curvature (which defines the transverse mode spectrum). The figure shows the 3MI gain as a function of frequency. Higher gain modes tend to cluster around the transverse mode offset frequencies. Those points with R>1 would normally be supressed to below unity for stable operation of the interferometer. If the radius of curvature changes or if the laser spot moves on the mirror, the points representing the parametric gain move up or down such as the examples discussed below. Typically, for a fused silica test mass for advanced detectors, we expect ~ 760 modes per test mass for R> 10^{-3}, and ~ 1000 modes per test mass in the negative gain range of R<-10^{-3}. The 3MI optical signal is equally detectable in the negative gain regime. The total number drops from ~1800 to ~700 for |R| >10^{-2}. These threshold values are chosen because they correspond to easy detectability at full power and 10% power respectively.

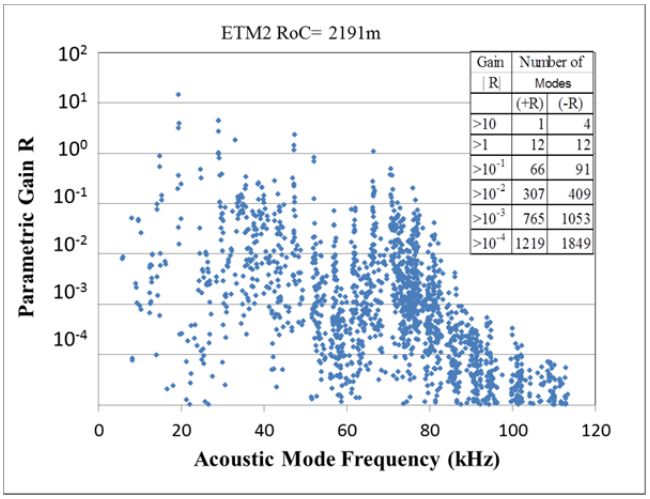

Figure 1. An example of acoustic modes showing the variability of parametric gain in a 4km dual recycling advanced gravitational wave detector configuration with fused silica ITM RoC=1971m and ETM RoC=2191m [21]. The acoustic modes are clustered in strips corresponding to cavity transverse mode offset frequencies. The cumulative number of acoustic modes (which is roughly the same across large range of RoC) is also given. All modes with gain > 10^{-3} should be easily detectable with a multi-element photodetector as discussed in text.

It is useful to calculate the magnitude of the wavefront distortions corresponding to the observed radius of curvature sensitivity discussed above. A change in radius of curvature translates to a fractional change in wavefront according to the simple geometric relation below.

$$\Delta d = \frac{r^2}{2R_m^{\,2}}\Delta R_m, \tag{3}$$

where R_m is the mirror radius of curvature, and r is the effective radius of the area of test mass where the laser effect dominates, and d is the depth of the mirror deformation. For an effective r ~ 5cm, and a radius of curvature of R_m~2000m, $\Delta d \sim 3\times10^{-10}\Delta R_m$.

Figure 2 shows typical model results for 3MI gain as a function of RoC for an advanced interferometer configuration with power recycling. It can be seen that some modes change their gain by several orders of magnitude over a few meters change in radius of curvature and some show asymptotic behaviour in which the gain can change by 100% in a few cm change in RoC.

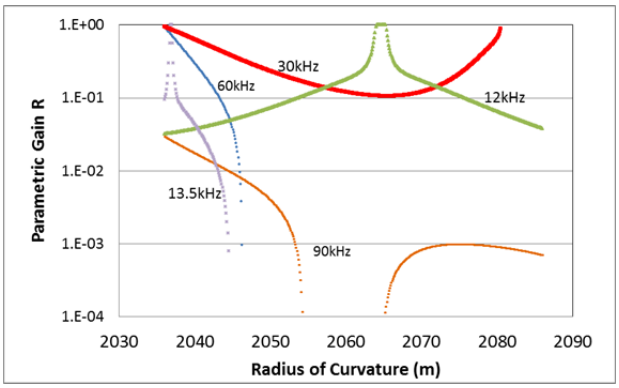

Figure 2. The parametric gain R as a function of mirror radius of curvature for several representative modes based on a power recycling advanced detector configuration over large radius curvature range.

We have analysed the available RoC sensitivity in modelling data corresponding to Fig 2, for both positive and negative gain modes. With the criteria of $|R|>10^{-3}$ and detectable gain change $\Delta R/R$ >10%, we found that 95% of the RoC range (2036-2086m) has modes sensitive to 10mm RoC change, corresponding to ~ $3\times10^{-6}\lambda$ (λ=1064nm), while 15% of the RoC range has modes sensitive to 2mm RoC change, corresponding to wave front error ~$6\times10^{-7}\lambda$. In this sense 3MI offers monitoring at an unprecedented precision. Hundreds of modes are always available with somewhat less sensitivity. However modelling that includes realistic mirror figure errors, plus observations, are needed to confirm the sensitivity of this monitoring tool.

4. Three mode interaction monitoring at Gingin facility

We have investigated 3MI in two different ~80m cavities at the Gingin High Optical Power Facility. The systems are rather simple. A cavity with high g-factor is locked by injected 1064nm TEM_{00} light. A quadrant photodetector monitors the transmitted beam. The south arm of the Gingin facility uses a cavity with sapphire test masses while the east arm uses fused silica test masses. Both cavities have allowed observation of 3MI.

The east arm system was designed specifically to study 3MI. It is a near concentric cavity similar to an Advanced LIGO arm cavity, with fused silica test masses 100mm diameter × 50mm thickness in a cavity of length 73.9m, and radii of curvature of 37.4 m and 37.5 m. The measured cavity finesse is 14500+/-300, and the cavity g-factor is ~0.98, leading to a transverse mode spacing from Eq. (2), of ~100kHz. This means that test mass acoustic modes at ~100 kHz can scatter the cavity fundamental mode into the cavity first order mode while acoustic modes near 200 kHz will scatter the fundamental mode into the second order mode, etc.

The 77m south arm was initially designed for thermal lensing and compensation studies[22]. The cavity has a flat input test mass (ITM) and a 720m RoC end test mass (ETM). It also provides an excellent test bed for controlled thermal tuning of 3MI as sapphire has much higher thermal conductivity than fused silica.

Modes with parametric gain ~10^{-3} are relatively easily observed. In the south arm sapphire test mass cavity, Zhao, *et al* observed a 3MI with R~ -0.01 and SNR of over 20dB, when the radius of curvature of the end test mass was appropriately thermally tuned [23]. Normally monitoring is done using a quadrant photodetector which is particularly sensitive to the TEM_{01} mode.

Figure 3 shows two examples of 3MI in those 2 cavities, one with a low cavity power and a controlled CO_2 laser thermally tuning the sapphire end test mass RoC in the south arm[24], the other with high cavity power and a spontaneous RoC change due to optical absorption in the east arm. In the case of controlled thermal tuning (fig 3a), acoustic mode thermal peaks appear with the change of the heating power. A few hundred milliwatts change in heating power is sufficient to sweep across the entire resonant peak. Typically the 3MI gain changes by a factor 3 as the heating power changes by ~100mW. In the case of RoC changes due to absorption (fig.3b), we observed 3MI similar to the CO_2 tuning as we increase the cavity power from 500W to 5kW in the fused silica east arm cavity. The carrier laser heating causes self-induced thermal aberration, thereby shifting the TEM_{01} mode frequency which determines the frequency at which acoustic modes are resonant.

Correlating CO_2 laser heating with 3MI observations provides an easy means of identifying the test mass associated which a particular acoustic mode. As discussed above the positive frequency tuning coefficient $\delta f/dT$ in fused silica test masses due predominantly to the temperature dependence of Young's Modulus (magnitude ~10^{-4} per degree) makes this easy and provides a powerful temperature probe. The high Q-factors of test mass modes allows mHz frequency resolution, corresponding to mK temperature resolution (depending on integration time). Because test masses are not normally in thermal equilibrium, the observed frequency depends on the acoustic mode shape. Thus measurement of the frequency of many modes allows estimates of thermal inhomogeneities at the mK level.

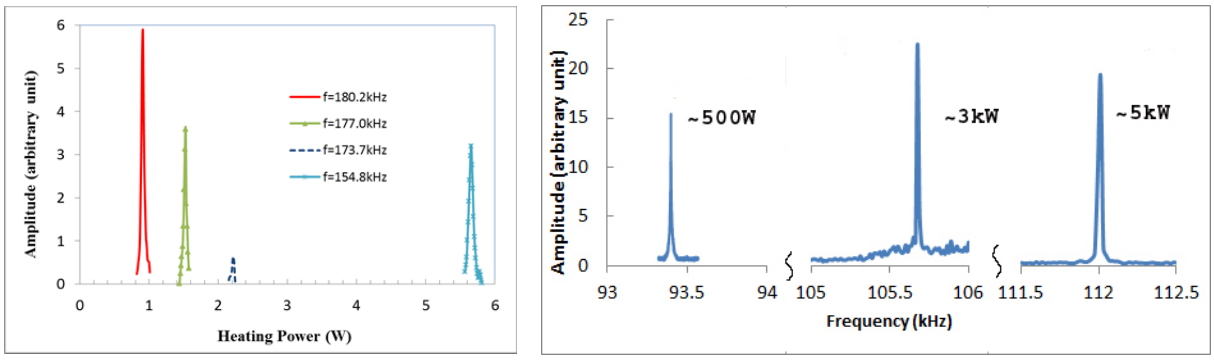

(a) (b)

Figure 3. Amplification of thermal peaks of test mass acoustic mode through 3MI. (a) Acoustic modes of a sapphire test mass in the south arm observed by controlled thermal tuning using a CO_2 laser. The CO_2 laser tunes the transverse mode frequency, thereby changing the 3MI condition. Peak height variations correspond to different overlap factors. (b) Three acoustic modes of a fused silica test masses, observed by 3MI at different cavity power levels. In this case the cavity transverse mode is tuned by optical absorption in the test masses, causing different acoustic modes to be resonant at different power levels.

Because the test masses in both cavities are relatively small, the acoustic mode density is low and instead of seeing a large number of modes simultaneously we observe modes only when the CO_2 laser power has correctly tuned the transverse mode frequency to allow a particular mode to be observed.

Another observation was that the position and size of the CO_2 laser spot significantly alters the 3MI signal. In this case we assume that we are observing inhomogeneous changes in the shape of the mirror which was distorting both the transverse mode shape and the mode frequency.

Without CO_2 heating and at a cavity power level of ~ 3kW, we observed that a few millimeters change in position of the laser spot on a test mass causes easily detectable changes in the 3MI signal, which is due to changes in the overlap parameter. This demonstrates the high sensitivity of the 3MI signal to laser beam alignments. This is expected because misalignment changes the position of optical anti-nodes relative to acoustic anti-nodes. Changes in overlap can cause large reductions in the overlap parameter such that some modes fall below the noise floor while different acoustic modes become visible. Another cause of the 3MI signal change could be due to the fact that mirrors in east arm are not of the highest quality so that beam spot misalignment would also incur cavity g-factors change due to the imperfection of the radii of curvature of the mirrors and inhomogeneous optical absorption. Thus it is possible to use relative mode amplitudes to diagnose changes of the optical cavity conditions such as g-factor, and spot position.

The above observations show the intrinsic high sensitivity of 3MI. They also show that the 3MI signals depend on multiple parameters – laser spot position, CO_2 laser heating position, and laser power. If only a few modes were available it could be very difficult to disentangle these various effects. However every 3MI signal has different dependences on these parameters. For example, higher order modes are more sensitive to spot position change than low order modes because cancellation of the overlap parameter occurs typically over half the dominant spatial wavelength. Test mass radius of curvature changes modulate the 3MI gain through high order mode detuning which is set by the optical transverse mode linewidth. Since these effects are independent, it is reasonable to expect that unique solutions should be available as long as a sufficient number of modes are monitored.

5. **Discussion and Conclusion**

Three mode interactions have not been previously observed in long baseline interferometers because the digital sampling rate on the photodetectors has been insufficient to observe the 10 - 100kHz frequency band in which these interactions occur. Since the modelling agrees with observations in the 80m cavities, we can be confident that with the use of appropriate signal detection 3MI signals will show up strongly in all long baseline interferometer cavities, even at low power.

Experimentally 3MI monitoring is simple, in the first instance by monitoring the transmitted light of interferometer cavities with a quadrant photo detector as discussed above. Such a detector would not be sensitive to all possible transverse modes but should allow the basic concepts to be verified, and difficulties identified. To optimise the 3MI signals a 3×3 or 4×4 photo detector should be used. Individual element outputs can be digitised and processed in linear combinations to optimise sensitivity to different optical modes. A single photodetector is usually insensitive to transverse mode signals because the spatially separated phases cancel out.

The high sensitivity of 3MI monitoring to small changes in test mass absorbed power has been demonstrated by both modelling and observations in two optical cavities. The high signal to noise ratio detection demonstrates the ability for low power measurements to predict modes likely to become unstable at high optical power in a single arm cavity. High power operation can easily be simulated by injecting appropriate CO_2 laser heating beams onto test masses as demonstrated in the Gingin south arm experiments.

Signals sensitive to both alignment and thermal perturbations (in a single cavity) were shown to be easily observed with signal to noise ratio of 10-20dB. We note that advanced interferometer alignment control is specified to be $\sim 10^{-9}$ radians, corresponding to ~4μm position change on the mirror. If mirrors are non-spherical transverse modes could be misaligned relative to the main beam. Such misalignments could increase or decrease the parametric gain depending on both the acoustic and transverse mode shapes.

In a more complex advanced interferometer the parametric gain depends on the Gouy phase associated with the entire coupled cavity configuration. The idealised modelling presented (that neglects the thermal compensation masses and optical inhomogeneities) shows that the method carries over to full dual recycling interferometers, but the large number of degrees of freedom means that disentangling the data will be a complex task as discussed further below.

Assuming some selection to account for frequency confusion and non-useful modes, multiple channels of data corresponding to hundreds of acoustic modes will first need to be identified with their test masses. Modes should appear in pairs, differing in frequency by parts in 10^{-4} due to dimensional differences between nominally identical pairs of inboard and end test masses respectively. Time dependent frequency differences will occur due to temperature changes. Thermal distortion will affect both signal amplitude and frequency, while alignment changes will change the signal amplitude without changing the frequency. Small angular dithering could also be used to separate thermal changes from alignment changes.

We propose that monitoring selected channels can allow improved control of high power interferometers, helping to predict and prevent parametric instability, and also possibly helping to minimize problems such as glitches that can occur due to the interaction of varying diameter beams with loss points on the mirrors, as well as drifts due to slow variation of the thermal profiles within the test masses.

However it is important to note that complete diagonalization (to allow extraction of individual error parameters in an advanced interferometer) will require identification and characterisation of a sufficient number of independent 3MI signals. Clearly experimental testing is required. Because there are so many acoustic mode channels there will be a need to determine which channels to use and how to combine them to create useful tools for separate purposes such as individual test mass thermal distortion detection and

compensation, or for diagnostics and control of potential instabilities. Substantial software development will be required.

Because 3MI signals are present all the time, initial experiments need only to record short stretches of data for later off-line analysis to begin to create a database of acoustic modes and mode frequencies. This could be undertaken at different stages of detector commissioning. Further work combining experiment and modelling will be required to match acoustic mode shapes to the observed frequencies, plus experiments to identify individual modes with their test masses, and to predict future instabilities. Once this work is done, it should be possible to develop software that will provide a real time monitor for global control of operating interferometers.

Acknowledgements

We thank the LIGO Scientific Collaboration (LSC), especially the LSC optical working group and Gregg Harry for the encouragement and discussions. We also thank the Gingin Advisory Committee of the LSC, chaired recently by Stefen Gossler for help and advice. This work is a project of the Australian Consortium for Interferometric Gravitational Astronomy (ACIGA) and was supported by the Australian Research Council.

References

[1] Aasi J, *et al*. (LIGO Scientific Collaboration and Virgo Collaboration) 2013 *Phys. Rev. D* **87** 022002
[2]Aasi J, *et al*. (LIGO Scientific Collaboration and Virgo Collaboration) 2013 *Nature Photonics* **7**, 613–619
[3] Braginsky V B, Strigin S E, and Vyatchanin S P 2001 *Phys. Lett. A* **287** 331-338
[4] Braginsky V B, Vyatchanin S P and Strigin S E 2002 *Phys. Lett. A* **305** 111-124
[5] Strigin S E, Blair D G, Gras S and Vyatchanin S P 2008 *Phys. Lett. A* **372** 5727-5731
[6] Gras S, Zhao C, Blair D G and Ju L 2010 *Class. Quantum Grav.* **27** 205019
[7] Zhao C, Ju L, Degallaix J, Gras S and Blair D G 2005 *Phys. Rev. Lett.* **94** 121102/1-4
[8] Ju L, Blair D G, *et al* 2004 *Class. Quantum Grav.* **21**, S887-S893
[9] Zhao C, *et al*. 2008 *Phys. Rev. A* **78** 023807
[10] Zhao C, Degallaix C, et al 2006 *Phys. Rev. Lett*. **96**, 231101
[11] Degallaix J, Zhao C, Ju L and Blair D G 2007 *J. Opt. Soc. Am*. **24**, 1336-1343
[12] Susmithan S, Zhao C, Fang Q, Ju L and Blair D G 2012 *Journal of Physics: Conference Series* **363**, 012018
[13] X. Chen, *et al* 2013 arXiv:1303.4561v2 [physics.optics]
[14] Gras S, Blair D and Zhao C 2009 *Class. Quantum Grav*. **26** 135012
[15] Fan Y, Merrill L, Zhao C, Ju L, Blair D, Slagmolen B, Hosken D, Brooks A, Veitch P and Munch J 2010 *Class. Quantum. Grav.* **27** 084028
[16] Gras S, 2013 http://space.mit.edu/symposium/postdoc/2013/gras.pdf
[17] Miller J, Evans M, Barsotti L, Fritschel P, MacInnis M, Mittleman R, Shapiro B, Soto J and Torrie C 2011 *Phys. Lett. A* **375** 788-794
[18] Evans M, Barsotti L and Fritschel P 2010 *Phys. Lett. A* **374**, 665-671
[19] Ju L, Blair D. G., Zhao C., et.al. 2006 *Class. Quantum Grav*. **26** 015002
[20] Ju L, Gras S, Zhao C, Degallaix J and Blair D G 2006 *Phys. Lett. A* **354**, *360-365*
[21] Gras S 2009 *Opto-acoustic interactions in high power interferometric gravitational wave detectors*, PhD Thesis, The University of Western Australia
[22] Degallaix J, Zhao C, Ju L and Blair D, 2004 *Class. Quantum Grav.*, **21** S903-S908
[23] Zhao C, *et. al* 2011 *Phys. Rev. A* **84**, 063836
[24] Susmithan S, Zhao C, Ju L, Fang Q and Blair D 2013 *Phys. Lett. A* **377** 2702–2708